NEUROSTIMULATION IN UPPER-LIMB AMPUTEES FOR SUPPRESSION OF PHANTOM LIMB PAIN: CHANGES IN HIGH-DENSITY EEG PATTERNS

Daria Kleeva
Vladimir Zelman Center
for Neurobiology and Brain Rehabilitation,
Skolkovo Institute of Science and Technology;
Moscow State University;
Moscow, Russia;

Gurgen Soghoyan
Vladimir Zelman Center
for Neurobiology and Brain Rehabilitation,
Skolkovo Institute of Science and Technology;
Moscow, Russia;

Artur Biktimirov
Laboratory of Experimental and Translational Medicine,
School of Biomedicine,
Far Eastern Federal University,
Vladivostok, Russia;
Motorica LLC, Moscow, Russia

Nikita Piliugin
Vladimir Zelman Center
for Neurobiology and Brain Rehabilitation,
Skolkovo Institute of Science and Technology;
Moscow, Russia;

Yury Matvienko
Motorica LLC,
Moscow, Russia

Mikhail Sintsov
Motorica LLC,
Moscow, Russia

Mikhail Lebedev
Faculty of Mechanics and Mathematics, Lomonosov Moscow State University,
Moscow, Russia;
I. M. Sechenov Institute
of Evolutionary Physiology and Biochemistry,
Saint Petersburg, Russia

August 13, 2023

ABSTRACT

Phantom limb pain (PLP) is a distressing and persistent sensation that occurs after the amputation of a limb. While medication-based treatments have limitations and adverse effects, neurostimulation is a promising alternative approach whose mechanism of action needs research, including electroencephalographic (EEG) recordings for the assessment of cortical manifestation of PLP relieving effects. Here we collected and analyzed high-density EEG data in three patients (P01, P02, and P03). Peripheral nerve stimulation (PNS) suppressed PLP in P01, but was ineffective in P02. By contrast, transcutaneous electrical nerve stimulation (TENS) was effective in P02. In P03, spinal cord stimulation (SCS) was used to suppress PLP. Changes in EEG oscillatory components we analyzed using spatio-spectral decomposition (SSD) and Petrosian fractal dimension (FD). With these methods, changes EEG spatio-spectral components were found in the theta, alpha, and beta bands in all patients, with these effects being specific to each individual. These changes in EEG patterns were found for both the periods when PLP level was stationary and the periods when PLP was gradually changing after neurostimulation was turned on or off. One consistent effect was an increase in EEG fractal dimension on the side contralateral to the amputation when PLP was present, while effective stimulation resulted in a decrease in fractal dimension. Overall, our findings align with the proposed roles of brain rhythms in thalamocortical dysrhythmia,

which is has been linked to neuropathic pain. The individual differences in the observed effects could be related to the specifics of treatment in each patient and the unique spectral characteristics in each of them. These findings pave way to the closed-loop systems for PLP management where neurostimulation parameters are adjusted based on EEG-derived markers.

Keywords phantom limb pain · EEG · peripheral nerve stimulation · spinal cord stimulation · neuromodulation · neuropathic pain

Introduction

Phantom limb pain (PLP) is a distressing and persistent sensation experienced after the amputation of a limb. The phenomenology of PLP is diverse, with common sensations including pressure, aching, burning, and spasms (McCormick et al., 2014). This condition has a significant impact on the quality of life of affected individuals, with the estimates of its prevalence reaching as high as 64 % (Limakatso et al., 2020), which underscores the need for effective management strategies.

Pharmacological treatment is the primary approach to managing PLP, with a range of medications available including beta-blockers, anaesthetics, opioids, NMDA receptor antagonists, muscle relaxants, nerve blocks, and others. However, the short- and long-term effectiveness of most of these medications is not well established. Even medications like morphine, gabapentin, or ketamine, which are associated with short-term pain relief, could have adverse side effects such as constipation, sedation, and respiratory problems (Alviar et al., 2016).

In light of the limitations of pharmacological interventions, neurostimulation is emerging as a promising treatment option to treat PLP, including spinal cord stimulation (SCS) and peripheral nerve stimulation (PNS). Both SCS and PNS activate afferents fibers while PNS is more selective to influence residual limb nerves (Petersen et al., 2019). Whereas the pain-relieving mechanisms of neurostimulation are not completely understood, several explanations have been proposed. According to the gate control theory (Melzack and Wall, 1965), the electrical stimulation of non-nociceptive large-diameter $A\beta$ fibers suppresses the pain signals transmitted to the spinal cord through the smaller $A\delta$ and C fibers by inhibiting interneurons involved in this transmission. In addition to the effects that the neurostimulation has on the spinal cord circuitry, higher hierarchical levels could be also engaged where neurostimulation-induced inputs reach cortical sensorimotor areas and offset the amputation-related remapping and pathological activity.

While the patients' subjective reports of the changes in PLP are used as the key criterion of treatment effectiveness, neurophysiological indicators could improve the assessment of treatment effects. Thus, using electroencephalography (EEG) as an objective marker of response to neurostimulation could significantly aid the treatment and lead to the development of closed-loop systems where neurostimulation parameters are adjusted based on EEG measurements. Better understanding of how EEG patterns correspond to different stages of PLP will facilitate the development of improved diagnostics, prognostics, and treatment monitoring for PLP, as well as optimizing current neurostimulation approaches.

EEG patterns are not sufficiently understood that could serve as biomarkers of pain. According to a recent review of EEG spectral characteristics in chronic neuropathic pain (Mussigmann et al., 2022), theta power grows consistently when pain increases. Studies on the involvement of alpha and beta rhythms have yielded mixed results, with some studies showing a correlation between the power in these bands and pain intensity and others reporting an opposite trend. These differences could be related to heterogeneity in the study designs: whether the eyes were open or closed, the specific frequency bands used in the spectral analysis, and other settings.

Several studies examined EEG patterns in amputees. In a case report (Walsh et al., 2015), the left frontal spectral power increased in a patient who attempted movements of the phantom limb, and these EEG modulations resembled the ones observed in healthy subjects during voluntary movements of their limbs. A study of the resting-state EEG network (Lyu et al., 2016) compared healthy controls to right-hand amputees. Alterations were found after limb amputations in the global and local phase synchronization of the alpha and beta rhythms. In a study of non-painful electrical stimulation of the limbs in amputees, stimulation of the affected limb resulted in an increase in the response of the N/P135 dipole (Vase et al., 2012). Additionally, alpha wave coherence increased with PLP reduction during virtual reality (VR) rehabilitation and vibrotactile stimulation of the referred sensation in the cheek and shoulder (Osumi et al., 2020). Using intracranial EEG recordings from the anterior cingulate cortex and orbitofrontal cortex, Shirvalkar et al. (2023) predicted the severity of chronic pain, including PLP. They found that while certain predictors showed some consistency (such as chronic pain being associated with orbitofrontal activity and acute pain with anterior cingulate cortex activity), the spectral characteristics and the weights of these features varied across patients, which hindered generalization to a wide population of patients.

Overall, the current knowledge of EEG correlates of PLP and other types of pain is insufficient for the development of efficient bidirectional systems for pain treatment. As a step toward the knowledge in this field, this study aimed to assess EEG patterns resulting from the treatment of PLP with PNS and SCS in three patients with upper-limb amputations.

Materials and methods

Participants

EEG data were collected in three upper-limb amputees: patients P01, P02, and P03. All three patients signed an informed consent. The experimental design was approved by the Ethical Committee of FEFU Biomedicine school (Protocol num. 4; April 16, 2021). The study was registered as a clinical trial num. NCT05650931 on the platform ClinicalTrials.gov. P01 and P02 had transhumeral amputations on the left side, and P03 had a transradial amputation of the right side. All patients experienced PLP at the level of 7-8 points estimated by a visual analogue scale (VAS).

Treatment

All patients were treated with neurostimulation, with individual differences in the stimulation sites and treatment strategies. PNS of the median nerve was effective to suppress PLP in P01, so this patient was treated with an ongoing PNS. PNS of the median nerve was ineffective in P02 but transcutaneous electrical nerve stimulation (TENS) was effective. In P03, spinal cord stimulation (SCS) was applied through the electrodes implanted over the segments Th6-7 to suppress PLP.

EEG recordings

EEG signals were sampled at 1,000 Hz with an NVX-136 amplifier. A 128-channel cap was used in patients P01 and P03. In patient P02, a smaller 60-channel cap was used because it fit the head better. The ground electrode was set to AFz. Ear clips were used as reference electrodes (positions A1 and A2) at the stage of data acquisition. Subsequently, the data were re-referenced to common average reference.

In all patients, resting-state EEGs were recorded with eyes open and closed during different stages of neurostimulation procedures, including stimulation being turned on or off and the associated states of PLP. Each patient received individual, neurostimulation-based treatment. Therefore, the arrangement of intervals where neurostimulation was on or off varied across the subjects. For each condition, the participants verbally described their sensations. The audio of these comments was recorded. For the nonstationary conditions where PLP was gradually changing after the stimulation was turned on or off, EEG recordings continued until the PLP level stabilized.

In patient P01, PNS continued throughout the day and was powerful enough to remove PLP completely. Accordingly, EEG recordings started with the stationary condition where PNS was still ongoing and no PLP was present. Next, after the eye-open and eye-closed data were collected, PNS was turned off. The subsequent EEG recordings corresponded to a nonstationary condition where PLP was gradually reappearing. After the patient reported that PLP stabilized, resting-state EEG was recorded for the PLP experienced in the absence of PNS. After this recording was completed, PNS was turned on, after which PLP was gradually disappearing.

In patient P02, EEG data were collected for both PNS, ineffective for PLP relief, and TENS which was effective. The PNS dataset contained data for three conditions: PNS on, PNS off, and PNS on again. The TENS dataset covered the following conditions: TENS off, TENS on, and TENS off again. Periods were documented where PLP was gradually decreasing after TENS was turned on and increasing after it was turned off.

Patient P03, in whom SCS was used to suppress PLP, was available only for one recording session. The patient took a pain-relieving medication on the night prior to the session, so no PLP was experienced in the beginning of the recordings although SCS was turned off. Next, while though there was still no PLP because of the medication effect, SCS was turned on. Finally, SCS was turned off, but this time the patient started to experience PLP.

EEG analysis

EEG was analyzed in MNE Python (Gramfort et al., 2013). The recordings were low-pass filtered (<30 Hz). Noisy and flat channels were discarded manually and interpolated where appropriate. The EOG, muscle, powerline, and neurostimulation artifacts were removed by the means of independent component analysis (ICA, FastICA algorithm). Next, we conducted a spectral analysis of the cleaned signals, which consisted of calculating the relative power spectral density using multitaper on 10-s segments of the EEG data.

To analyze the changes in oscillatory components of interest, we conducted spatio-spectral decomposition (SSD) (Nikulin et al., 2011). This method involves a linear decomposition of multichannel EEG data which optimizes the signal-to-noise ratio by maximizing the peak-frequency power and minimizing it for the neighboring bands.

Because of the variability in the EEG spectral profiles across the participants, we assessed the EEG patterns with the appropriate for such cases metric called Petrosian fractal dimension (FD) (Petrosian, 1995) , which was computed on 30-s EEG segments. The Petrosian FD was computed as:

$$P = \frac{\log_{10}(N)}{\log_{10}(N) + \log_{10}(\frac{N}{N + 0.4N_\delta})}, \tag{1}$$

where N is the length of a time series for a single EEG channel, and N_δ denotes the count of sign changes in the derivative of the signal. This approach was developed for the estimation of EEG signal complexity. The FD measure matches well the other complexity metrics such as different types of entropy and Lempel-Ziv complexity.

Statistical analysis

Since we analyzed each patient individually and the spectral properties of resting-state EEG were variable across the conditions, we did not explicitly divide power spectral density (PSD) into frequency bands. In order to determine PSD segments with statistically significant changes, we used a permutation cluster test Maris and Oostenveld (2007), which resolved the multiple comparisons problem for the features in question (a set of frequencies and channels). In this test, the cluster-forming threshold was set to 0.025 for the observed t-values because the statistics was two-tailed. The number of permutations was set to 10^3. Statistical significance level was set to $p < 0.05$ for the cluster of frequencies and channels. To account for multiple comparisons across different conditions, we adjusted the p-values by applying the Bonferroni correction.

To analyze EEG patterns for the cases where PLP changed gradually, we used a Mann-Kendall test, which detected the features characterized by significant monotonic trends.

Results

Subjective reports

The subjective experiences of each patient were highly individual. In patient P01, PNS strongly suppressed PLP with some day to day variations. On the day when EEG recordings were conducted in this patient, PLP was suppressed by 90%. In the absence of PNS, the patient felt PLP. The PLP was accompanied by a sensation of compression. Both of these sensations were suppressed by PNS. PNS evoked non-painful sensations itself in the phantom which were localized to the left palm, in the area of the dermatome C6.

In patient P02, both PNS and TENS was tested. On the PNS testing day, PLP was felt in the right little finger and the right wrist. PNS induced sensations in the phantom forearm, in the area normally innervated by the right lateral antebrachial cutaneous nerve. Yet, it did not suppress PLP. On the TENS testing day, the patient reported PLP suppression by 60 % by TENS in the right little finger and the right bend of the elbow. The TENS evoked phantom sensations at the base of the right thumb.

In patient P03, PLP was felt over the entire left palm. SCS evoked sensations in the same area of the phantom and suppressed PLP by 10-30 %, depending on the day of treatment. On the day when EEG recordings were conducted, the patient took medication which abolished PLP completely, but during the last recording session when the SCS was turned off, PLP returned to the usual level.

Spatio-spectral characteristics

The analysis of the EEG spatio-spectral characteristics revealed across-condition modulations. Figure 1 shows the results of the PSD analysis for the eyes-open condition. Significant changes were found for eight spatio-spectral clusters.

One noticeable change for the eye-open condition, was the presence of a prominent alpha peak after PNS was turned off. The PSD analysis attributed this effect to cluster 4 (115 channels, mean t-value = 2.701), which revealed a spatially widespread increase in the alpha power in the frequency range 8.4-10.9 Hz. Mean PSD increased from 0.0053 ±0.001 to 0.0068 ±0.0021. While alpha activity increased in both hemispheres, this effect was somewhat stronger in the left anterior regions (i.e. ipsilateral to the amputation) and the right posterior regions.

While the alpha power increased, decreases occurred in the theta (clusters 1 and 2) and low beta power (cluster 3). Cluster 1 (39 channels, mean t-value = 2.263) was localized over the left frontal areas. For this cluster, significance changes were detected in the frequency range 6.1-8.1 Hz. Mean PSD decreased from 0.0073 ±0.0013 to 0.0063 ±0.0012 occurred in the frequency range 6.1-8.1 Hz. Cluster 2 (20 channels, mean t-value = 2.706) was localized over the right parietal areas. For the frequency range 6.5-7.9 Hz, mean PSD decreased from 0.0077 ±0.0018 to 0.0064 ±0.0015. Cluster 3 (92 channels, mean t-value 1.917), corresponded to a spatially widespread decrease in low beta power (12.3-17.5 Hz). Mean PSD decreased from 0.0036 ±0.00083 to 0.0031 ±0.00047) for the frequency range 12.3-17.5 Hz.

Additionally, clusters 5 and 6 corresponded to an increase in high beta power. Cluster 5 (24 channels, mean t-value = -2.24) covered the left frontal areas. Mean PSD increased from 0.00080 ±0.00018, to 0.001 ±0.00039 in the frequency range 24.8-30 Hz. Cluster 6 (61 channels, mean t-value = -2.168) had a broad contralateral localization. For this cluster, mean PSD increased from 0.00087 ±0.0002 to 0.0011 ±0.00047 in the frequency range 24.8-30 Hz.

When patient P01 closed the eyes, the alpha rhythm prominently increased. Two clusters, clusters 7 and 8, had significant changes after PNS was turned off. The frequencies where significant changes were detected were not higher than the frequency of the alpha oscillations. For Cluster 7 (N=104, mean t-value = -2.498) a generalized increase in the higher range of the alpha band (11.5-12.5 Hz) was found. Mean PSD increased from 0.00068 ±0.0035 to 0.0085 ±0.0036. For cluster 8 (N=38, mean t-value = -1.875), an increase in the high beta power (22.5-30 Hz) was found in the frontal areas ipsilateral to the amputation, which resembled the changes for cluster 5 in the eyes open condition. Mean PSD increased from 0.00047 ±0.00015 to 0.00058 ±0.00028.

In summary, resting-state EEG patterns changed in patient P01 after the PNS was turned off and PLP returned. Most notably, alpha oscillations increased for the eyes open condition. Additionally, also when the eyes were open, decreases in theta and low-beta activity occurred, as well as increases in high-beta activity. During the eyes closed conditions, alpha activity was elevated when the PNS was both on and off; more so for the the high-alpha frequencies when the PNS was off.

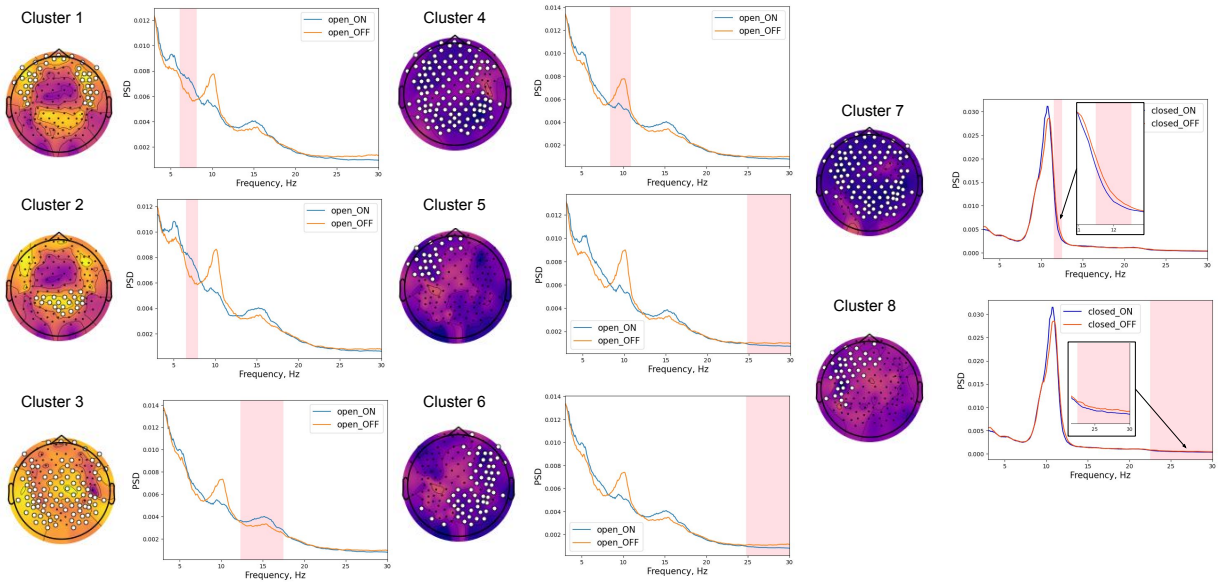

Figure 1: Spatio-spectral clusters in patient P01 with significant changes after PNS was turned off and PLP returned. Frequency intervals with significant changes in spectral power are shaded in pink; EEG channels, forming the clusters with significant differences, are marked with white dots. Scalp topographies depict the t-values. Clusters 1-3 represent simulation-related increase in theta and low beta power, clusters 4 and 7 represent pain-related increase in alpha power, and clusters 6-8 represent pain-related increase in high beta power.

We also observed gradual changes in EEG patterns in patient P01 occurring after PNS was turned off or on. These changes matched the gradual changes in PLP that the patient reported. To quantify the gradual changes in EEG, we examined the mean PSD for the presence of linear trends within the frequency bands identified in the analysis of spatio-spectral clusters. First, we analyzed the time course of alpha power, which was elevated in the absence of PNS. We identified a significant increasing trend for 92 channels (mean slope: 8.498e-06, mean intercept: 0.0047) (Figure 2, 1.A). These channels matched the channels with the alpha-rhythm increase identified in the analyses of epochs with the

stationary level of PLP (clusters 4 and 7 in Figure 1). Notably, a sharp increase occurred in the alpha rhythm toward the end of the nonstationary period. Yet, even when the period of this change was excluded the trend remained evident, (Figure 2, 1.B). For this shorter analysis epoch, 13 channels had a significant increasing trend (mean slope: 8.634e-06, mean intercept: 0.0045), and the majority of these channels were located in the anterior cortical regions.

A linear trend was also found for the low beta power. Mean PSD gradually decreased (mean slope: -4.556, mean intercept: 0.0036) for 79 channels after PNS was turned off (Figure 2, 1.C). This trend was also present after the period of sharp alpha increase was excluded from the analysis (mean slope: -3.557e-05, mean intercept: 0.006). This early trend was significant for 8 channels that corresponded to lateral posterior sites ipsilateral to the amputation and temporal sites contralateral to the amputation (Figure 2, 1.D).

Gradual changes in EEG patterns were also found for the condition where PNS was turned on following the period during which PLP fully returned. The patient reported that PLP was relieved in 5 min after PNS onset. During this period, a significant decrease in alpha power (mean slope: -6.874e-05, mean intercept: 0.0068) was observed for 34 channels representing the anterior and posterior regions (Figure 2, 2.B). Additionally, a significant gradual increase occurred in low beta power (mean slope: 5.812e-05, mean intercept: 0.0025) as evident from the data of 89 channels primarily localized in posterior scalp regions (Figure 2, 2.A).

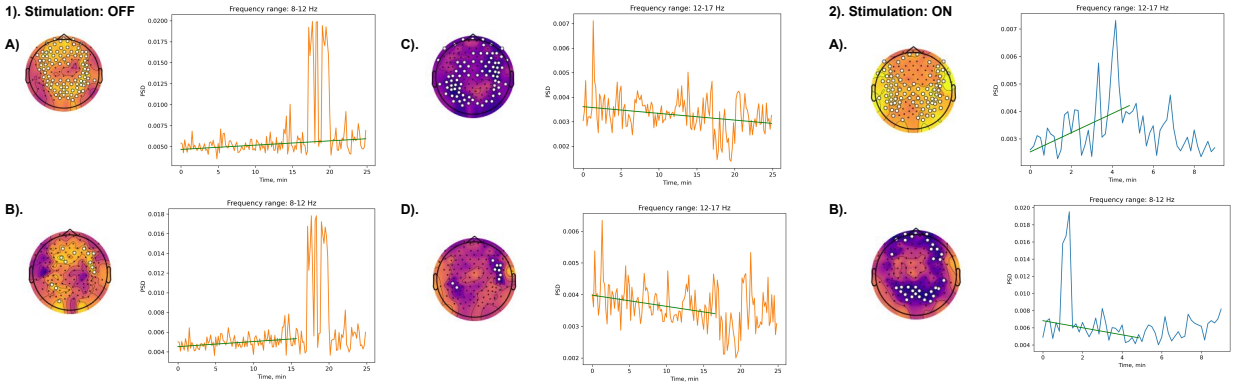

Figure 2: Gradual changes in mean PSD for different frequency ranges in patient P01 induced following PNS offset (A) and onset (B). Green line indicates the mean trend, channels at which significant trends were observed are marked with white dots. Scalp topographies depict Kendalls Tau value.

In patient P02, we analyzed the changes in EEG patterns for both TENS, which was effective to relieve PLP, and PNS, which was ineffective. In this patient, the power spectral density (PSD) exhibited peculiar characteristics, with a prominent beta component ranging from 10 to 30 Hz and a peak at around 6-8 Hz, which could have represented theta activity. The comparison of the TENS on and TENS off conditions showed that the 6-8 Hz peak was stronger in the absence of TENS, that is when PLP was present (Figure 3). This effect was evident for the frontally located cluster 2 (17 channels, mean t=-3.109) whose mean PSD for the 5.7-8.3 Hz frequency interval was 0.00336 ±0.00053 versus 0.00273 ±0.00043 for TENS on and TENS off conditions, respectively, and for the parietal and occipital cluster 3 (11 channels, mean t-value -3.88) with the mean PSD for 5.7-6.8 Hz being 0.005 ±0.0011) versus 0.00387 ±0.00096. PNS, although being ineffective for relieving PLP, had an effect on the EEG patterns in a broad frequency range from 3 to 15 Hz. Here, cluster 5 (35 channels, mean t-value -0.416) had significant differences for the interval 3-14.9 Hz: mean PSD was 0.00427 ±0.00022 in the absence of PNS and 0.00422 ±0.00035 in the presence of PNS.

The prominent beta activity also changed in patient P02 depending on the presence of neurostimulation. Stimulation-related effects were found for high beta power 25-30 Hz, which increased at the anterior and posterior sites as was evident from cluster 1 (43 channels, mean t-value 3.5654) where significant changes were found for frequency interval 25.2-30 Hz. For this cluster, mean PSD was 0.00159 ±0.0003 when TENS was applied, which decreased PLP, and mean PSD was 0.00122 ±0.00021 in the absence of stimulation. Additionally, cluster 4 (57 channels, mean t-value 1.627) exhibited a generalized increase in PSD for a rather wide interval from 17.7 to 30 Hz when PNS was applied even though no decrease in PLP was reported by the subject. Mean PSD was 0.00286 ±0.00032 in the presence of PNS and , 0.00266 ±0.00021) in the absence of PNS.

A comparison of the EEG patterns recorded during TENS to the those recorded during PNS showed differences for several frequency intervals. The activity for the interval 3 to 9.8 Hz was significantly higher during TENS than during PNS for the posterior sites that formed cluster 6 (30 channels, mean t-value 0.677). For this cluster, mean PSD was 0.00332 ±0.00048 for TENS and 0.00318 ±0.00035 for PNS. Additionally, cluster 8 (36 channels, mean t-value

= -1.371) showed a higher PSD during TENS in somewhat narrower frequency range 3 to 8.6 Hz. Mean PSD was 0.00277 ±0.00036 for TENS and 0.00303 ±0.00039 for PNS. Furthermore, cluster 7 (44 channels, mean t-value = 1.063) revealed an elevation in high beta power (22.1-30 Hz) when TENS was applied. Mean PSD was 0.00192 ±0.00032 for TENS versus 0.00182 ±0.00031 for PNS. Finally, activity was stronger for PNS than for TENS in a wide interval 18.4-30 Hz. The corresponding cluster, cluster 9 (11 channels, mean t-value -1.0414) was located ipsilaterally to the amputation. Mean PSD was 0.0027 ±0.0004 for PNS and 0.0029 ±0.00037 for TENS.

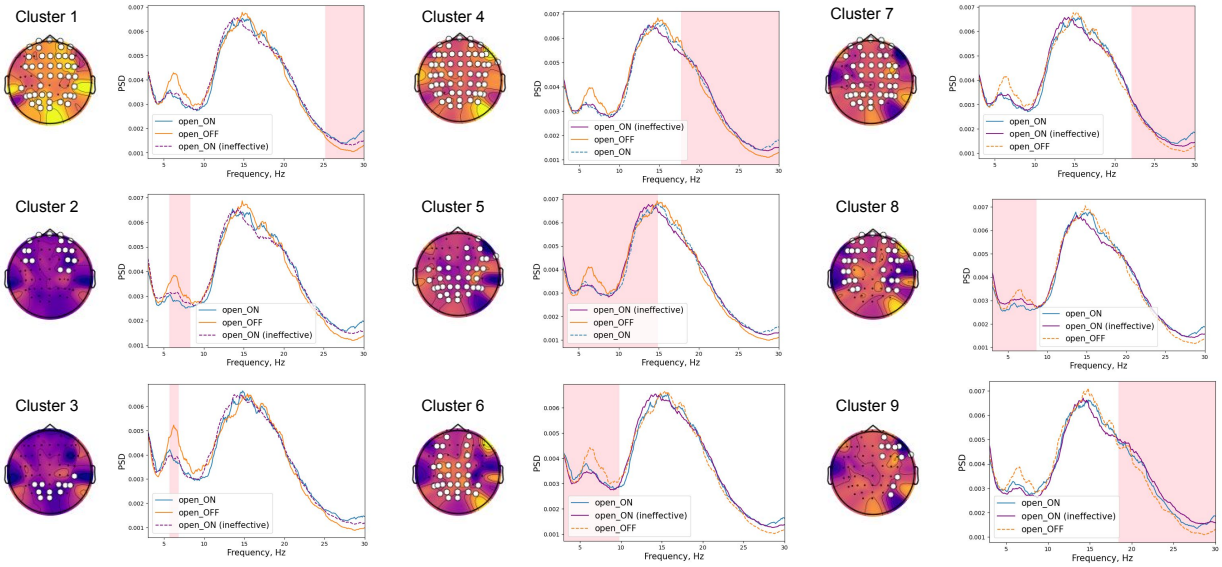

Figure 3: Spatio-spectral clusters in patient P02 with significant differences related to the presence of TENS or PNS. Data for the eyes-open condition are shown. Frequency intervals with significant changes in spectral power are shaded in pink. EEG channels, forming the clusters with significant differences are marked with white dots. Scalp topographies depict the t-values. For comparison purpose, dashed lines represent the data for the conditions that were entered in the statistical analysis. Clusters 1-3 had significant differences for TENS vs no stimulation, clusters 4-5 had differences for PNS vs no stimulation, and clusters 6-9 had differences for TENS vs PNS

.

For the eyes-closed condition, spectral changes were also found that depended on the presence of PNS or TENS (Fig. 4). Similar to the eyes-open condition, increased power was observed during TENS for the theta range, which could also represent a slow alpha variant. This effect was evident in the interval 3 to 5.6 Hz for cluster 1 (30 channels, mean t-value 2.71) with mostly posterior locations. For this cluster, mean PSD was 0.00247 ±0.00087 for TENS and 0.00197 ±0.00036 for the absence of stimulation. Cluster 2 (11 channels, mean t-value 3.341) showed an increased power during TENS for the interval 7-8.4 Hz. Mean PSD was 0.00266 ±0.00066 for TENS and 0.00212 ±0.00046 for the ansence of TENS. Cluster 5 (58 channels, mean t-value = 1.791) showed an increase activity during PNS for the inteval 3.0-13.5 Hz. Mean PSD was 0.00425 ±0.00064 for PNS and 0.00386 ±0.00042) for no stimulation. Additionally, cluster 9 (38 channels, mean t-value = -1.961) had had higher activity during TENS than during PNS in the interval 3-8.7 Hz. Mean was PSD 0.00242 ±0.00051 for TENS and 0.00277 ±0.00083 for PNS.

We also found in patient P02 increases in high beta power during both TENS and PNS. For cluster 3 (58 channels, mean t-value 3.455), an elevated activity was found in the interval 19.8-30 Hz during TENS(0.00235 ±0.00041) as compared to the absence of TENS (0.00188 ±0.00032). For cluster 8 (57 channels, mean t-value 2.355), mean PSD in the interval 14.4-30 Hz was higher during TENS (0.00347 ±0.00044) than during PNS (0.00311 ±0.00042). For cluster 6 (54 channels, mean t-value 1.1), PNS significantly increased high beta power in the interval 19.7-30 Hz as compared to an absence of stimulation. Mean PSD was 0.0021 ±0.00049 during PSD and 0.00191 ±0.00032 in the absence of stimulation.

Finally, TENS decreased power in the low beta band. Cluster 4 (56 channels, mean t-value -2.351) had lower activity in the interval 10.7-16.9 Hz during TENS (0.00639 ±0.00097) compared to the absence of stimulation (0.00754 ±0.00077). Cluster 10 (53 channels, mean t-value -2.107) had a lower activity in the interval 10-14.9 Hz during TENS (PSD 0.00608 ±0.0012) than during PNS (0.00709 ±0.0014). Cluster 7 (58 channels, mean t-value -1.749) showed that PNS slightly decreased power in the interval 12.7-21 Hz. Mean PSD was 0.0055 ±0.00086 during PNS and 0.00613 ±0.00044 in its absence.

It should be noted that PSD of patient P02 manifested non-trivial modulations in the low-beta range, which are more typical for the alpha range. As evident from cluster 11 (58 channels, mean t-value 2.238), low-beta power (9-18.2 Hz) was increased when the eyes were closed (mean PSD 0.0065 ±0.000472) compared to eyes-open condition (mean PSD 0.00541 ±0.000420). Additionally, we observed a theta power (3-10.2 Hz) decrease when eyes were closed. Cluster 12 (56 channels, mean t-value -4.541) had mean PSD decreased from 0.00334 ±0.000375 in the eyes-open condition to 0.0024 ±0.000244 in the eyes-closed condition.

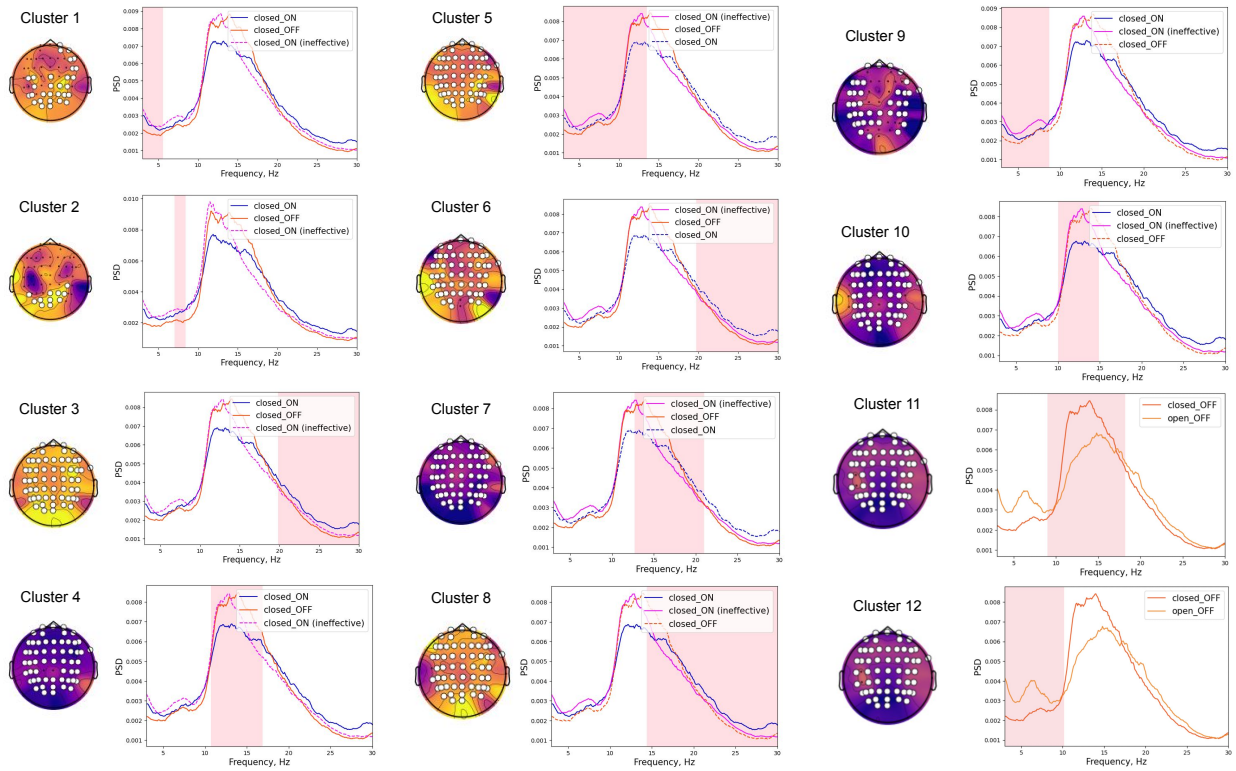

Figure 4: Spatio-frequency clusters with significant across-condition differences in patient P02 for thr eyes-closed condition. Frequency intervals with significant changes in spectral power are shaded in pink. EEG channels forming the clusters with significant differences are marked with white dots. Scalp topographies depict the t-values. For comparison purpose, dashed lines represent conditions that were not included in the particular statistical analyses. Clusters 1, 2, 5 and 9 reflect stimulation-induced modulation in theta power. Clusters 3,8, 6 correspond to changes in high beta power. Clusters 4, 7, 10 are the clusters with changes in low beta power. Clusters 11 and 12 depict the spectral differences in eyes-open and eyes-closed conditions

.

Like in patient P01, the analyses of gradual changes in EEG patterns in patient P02 showed significant trends for the periods following neurostimultaion onset or offset. The observed trends in gradual pain suppression or increase were associated with the modulation of theta power (Fig. 5). When the stimulation was turned off and the pain intensified, theta power gradually increased in 34 channels (mean slope 3.52e-05, mean intercept 0.00362) (see Fig. 5 1.A). Conversely, it decreased (mean slope -5.219e-06, intercept 0.00355) mostly at the sites ipsilateral to the amputation (22 channels in total), when stimulation was turned on (Fig. 5 2.A). Notably, during the last several minutes of the recording, this decrease was most pronounced, affecting a total of 43 channels (mean slope -3.246e-05, mean intercept 0.004) (Fig. 5 1.B).

In patient P03 (Fig. 6) (who for some period of time experienced pain suppression without stimulation due to analgetics), EEG patterns changed in association with SCS being turned on or off or irrespective of SCS. For the eyes-open condition, the pain-related effects were observed at fronto-central sites ispilateral to the amputation. For cluster 1 (23 channels, mean t-value = 1.9), a PSD decrease was observed for the range 3-8.9 Hz when SCS was turned off and the patient felt PLP. Mean PSD was 0.00744 ±0.0014 when SCS was on and PLP was absent, and 0.00616 ±0.0013 when SCS was off and PLP was present. For cluster 4 (21 channel, 3-8.3 Hz, mean t-value -2.513), that demonstrates the comparison of pain presence and pain absence, when the stimulation was turned off, PSD decreased, when the pain was present. Mean PSD fell from 0.00637 ±0.0015 to 0.0081 ±0.001. Additionally, a pain-related

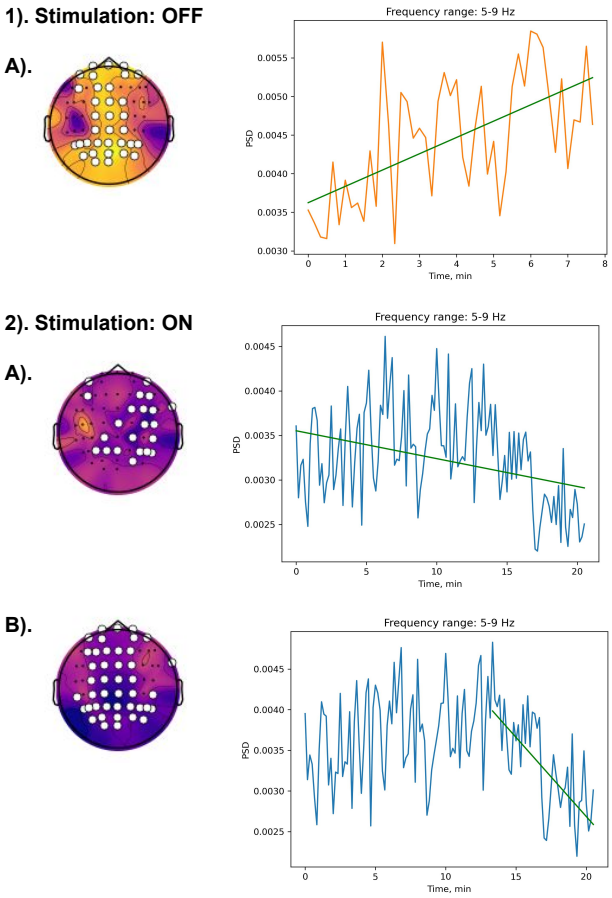

Figure 5: Gradual changes in mean PSD for different frequency ranges in patient P02 during the period when PLP increased after TENS was turned off (A) and decreased after TENS was turned on (B). Green line indicates the mean trend. Channels with significant trends are marked with white dots. Scalp topographies depict Kendalls Tau value.

increase in broad beta power (14-30 Hz) was observed. For cluster 2 (33 channels, 14.3-30 Hz, mean t-value -1.677), mean PSD grew from 0.00232 ±0.00049, to 0.00272 ±0.00059, and for cluster 3 (40 channels, 13.8-30 Hz, mean t-value 1.798), from 0.00263 ±0.00054 to 0.00221 ±0.00035.

For the eyes-closed condition, SCS modulated EEG patterns even without modulating PLP. An increase in PSD was observed for low EEG frequencies when SCS was turned off. For cluster 6 (109 channels, 3.3-8.4 Hz, mean t-value -1.025), mean PSD increased from 0.00557 ±0.00097 to 0.00643 ±0.0013, and for cluster 8 (125 channels, 3-8 Hz, mean t-value -2.544), from 0.00564 ±0.0012 to 0.00685 ±0.0012. Additionally, alpha power decreased. For cluster 5 (91 channel, 8.9-10.5 Hz, mean t-value = 2.217), mean PSD decreased from 0.0142 ±0.0055 to 0.0114 ±0.0051, and for cluster 7 (125 channels, 7.4-11.8 Hz, mean t-value = 1.573) , from 0.0096 ±0.00011 to 0.0.00806 ±0.0021.

Notably, in patient P03, turning SCS off evoked similar changes in the EEG patterns during the eyes-open and eye-closed conditions. When the pain was present, PSD decreased for the low EEG frequencies, as was evident from cluster 11 (21 channels, 3-6.6 Hz, mean t-value -2.409), and cluster 12 (38 channels, 3-6.4 Hz, mean t-value -2.209) data. For cluster 11, mean PSD decreased from 0.00642 ±0.0016 to 0.00789 ±0.0014, and for cluster 12 – from 0.00544 ±0.0018 to 0.0067 ±0.0017. Additionally, an increase was observed in beta power. For cluster 10 (8 channels, 16.7-30 Hz, mean t-value = 2.782), mean PSD increased from 0.00188 ±0.00029 to 0.0023 ±0.00031. Additionally, we observed an pain-related increase in lower part of alpha band. As was evident from cluster 9 data (23 channels, 7.3-8.7 Hz, mean t-value 2.759), mean PSD increased from 0.00644 ±0.0015 to 0.00795 ±0.0022.

SSD patterns

To investigate the potential sources of the identified spatio-frequency components, we conducted a spectro-spatial decomposition (Fig. 7). This analysis showed that the theta-frequency components observed in participants P01 and

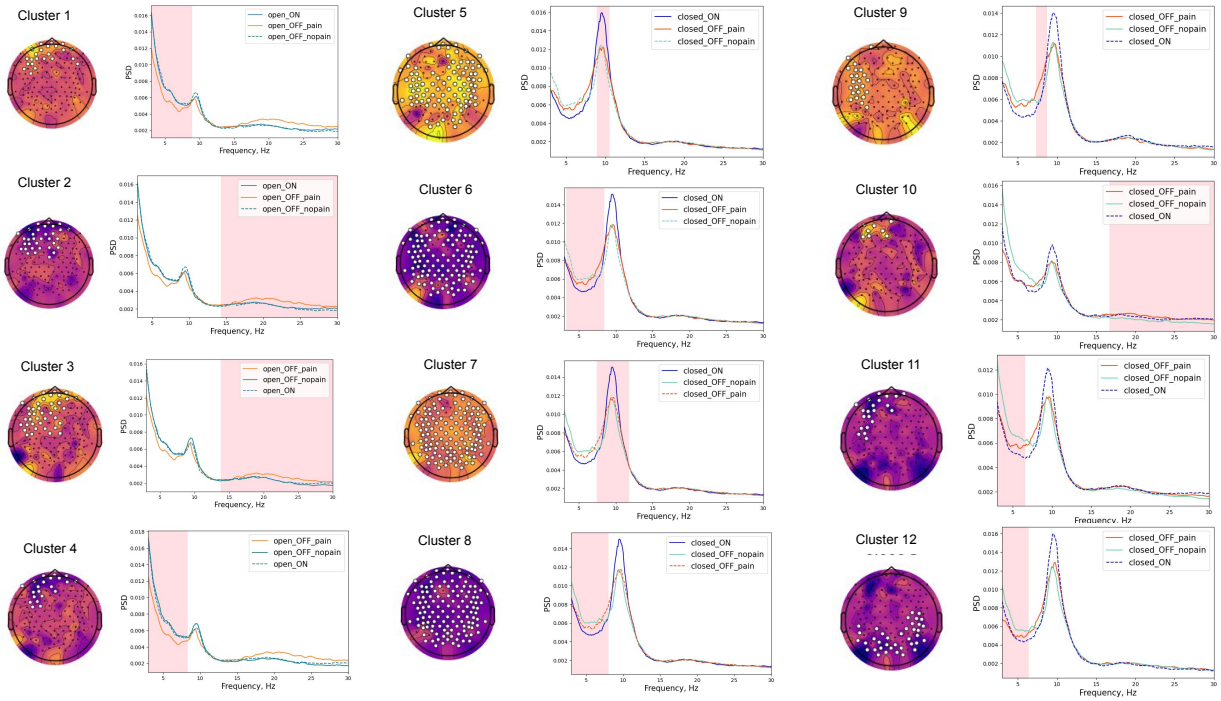

Figure 6: Spatio-frequency clusters with significant changes associated with the presence or absence of SCS in patient P03. Frequency intervals with significant changes in spectral power are shaded in pink. EEG channels forming the clusters with significant differences are marked with white dots. Scalp topographies depict t-values. For comparison purposed, the dashed line represents the conditions that was not used in the particular statistical analyses

.

P02 (Fig. 7 1.A and 2.A) and alpha activity in patient P03 (Fig. 7 3.A). originated from the parieto-occipital regions. Furthermore, low beta activity in patient P01, which increased during PNS, was localized in the occipital regions contralateral to the amputation (Fig. 7 1.C). Yet, beta activity in patient P03 who experienced PPL when SCS was turned off was localized to the fronto-temporo-central regions ipsilateral to the amputation (Fig. 7 3.B). Notably, in patient P01, the localization of alpha activity was contralateral to the amputation in the presence of PPL (Fig. 7 1.A). Additionally, patient P02 had a distinctive pattern where low-beta oscillations were localized in temporal regions contralateral to the amputation upon the onset of TENS, whereas in the other cases these oscillations were predominantly located in parieto-occipital regions (Fig. 7 2.B).

Fractal dimension

Fractal dimension (FD) analysis assessed EEG signal complexity (Fig. 8). In patients P01 and P03, PLP in the absence of neurostimulation was associated with an increase of FD at the sites contralateral to the amputation. Figure 8.1 shows patient P01 data (54 channels, mean t-value -2.987) where mean FD was 1.00365 ±7.583e-05 when PNS was on and 1.00378 ±0.000121 when PNS was off. For patient P02 (33 channels, mean t-value 3.989), mean FD was 1.00182 ±8.403e-05) 1.00191 ±4.703e-05 during TENS and 1.00182 ±8.403e-05) when TENS was off (Fig. 8.2). In this patient, TENS resulted in a decrease of FD (7 channels, mean t-value -4.523) contralaterally to the amputation (Fig. 8, 3.A). Mean FD was 1.00165 ±3.601e-05 during TENS and 1.00172 ±1.325e-05 when TENS was off. Figure 8, 3.B shows a comparison of the effects of TENS to PNS in Patient P02 (23 channels, mean t-value -6.459). Mean FD was 1.00169 ±3.136e-05 during PNS and 1.00177 ±3.242e-05 during TENS.

Discussion

In this study, we investigated the effects of PLP-relieving neurostimulation on the EEG patterns in three amputees. Resting-state EEG was recorded in several conditions, including PLP presence in the absence on neurostimulation, its absence in the presence of neurostimulation and a case of neurostimulation which was not effective to relieve PLP (PNS in P02). Overall, distinct EEG patterns were found for each condition, with a number of individual differences.

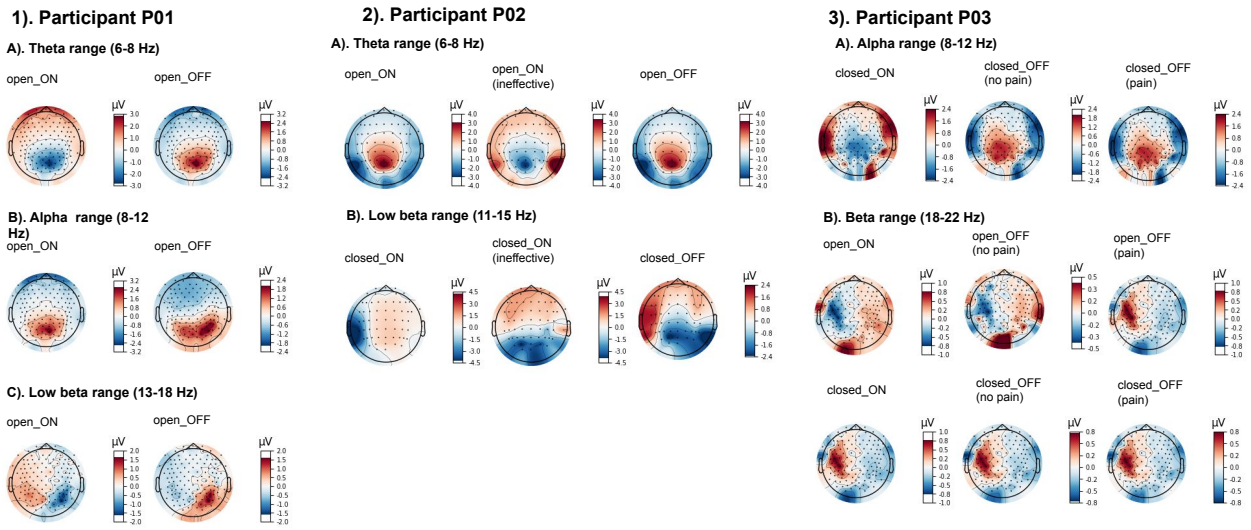

Figure 7: Spatial patterns in frequency bands for each participant and condition

.

EEG of each patient exhibited unique characteristics in terms of power spectrum density (PSD) and its modulations related to the presence of neurostimulation and its efect on PLP. Having the eyes open or closed also contributed to the individual variability.

The neurostimulation/PLP-sensitive EEG components were widespread over the cortical surface rather than corresponding to focal somatosensory or motor representations. Despite the across-participant variability, several common effects were observed, which were consistent with the previous literature. Thus, beta-band activity was elevated in the frontal regions ipsilateral to the amputation in two patients (P01 and P03) during the presence of PLP. In patient P01 this elevation was observed in the range 25-30 Hz and in patient P03 in the range 18-30 Hz. These findings match the previous reports of increased high-beta activity in different pain syndromes (Vanneste et al., 2017; Wang et al., 2019). Such an increased beta activity could reflect an alteration in the descending pain inhibition pathway linked to lateral prefrontal regions (Bräscher et al., 2016).

In each patient, we observed distinct and specific effects manifesting the neurostimulation and PLP conditions. Thus, increases in alpha power were prominent in patient P01 during the presence of PLP. PLP in patient P01 was accompanied with a feeling of stiffness, which bears relevance to the report of Simis et al. (2022a), where alpha band activity and stiffness were positively correlated in patients with osteoarthritis, which could reflect the influence of cortical inhibition due to peripheral damage. Furthermore, studies of peripheral neurogenic pain revealed modulations of the resting-state alpha or theta activity (Sarnthein et al., 2006; Olesen et al., 2011; van den Broeke et al., 2013). Similar EEG changes were observed for non-neuropathic painful conditions (Case et al., 2017; Fallon et al., 2018; Dinh et al., 2019), although some of them were related to pain chronification rather than pain intensity per se.

Thalamocortical dysrhythmia is one explanation for the alterations in theta and alpha rhytms in nociception (Jeanmonod et al., 2001). According to this framework, transfer of thalamic bursts of activity to the cortex acts as an abnormal painful input. This framework usually considers theta oscillations alone. However, since the alpha rhythm is a part of activity in thalamocortical loops, this explanation could be extended to the alpha range, as well. In this respect, the absence of alpha activity and prominent low-beta modulations observed in patient P02 could also represent thalamocortical oscillations altered during the presence of PLP. An increase of low-beta power during the eyes closed condition in this patient suggests that this activity could have been a shifted alpha rhythm. On the other hand, this could have also been the result of the edge effect (Llinás et al., 1999), where high-frequency oscillations are generated because of a pronounced pathological low-frequency activity. In patient P02 this low-frequency activity could have been represented by a pronounced theta peak. Similar increase in the theta and beta oscillations have been reported in patients with chronic pain (Zebhauser et al., 2023). Thus, in patient P02, TENS could have suppressed an abnormal low-frequency thalamocortical activity.

Changes in alpha activity, which is usually the most prominent EEG oscillation, were also observed. In patient P01, alpha power decreased during PNS, and this decrease was accompanied by an increase in low-beta activity (12-17 Hz). The latter effect is consistent with the previous literature that reported suppression of beta oscillations,

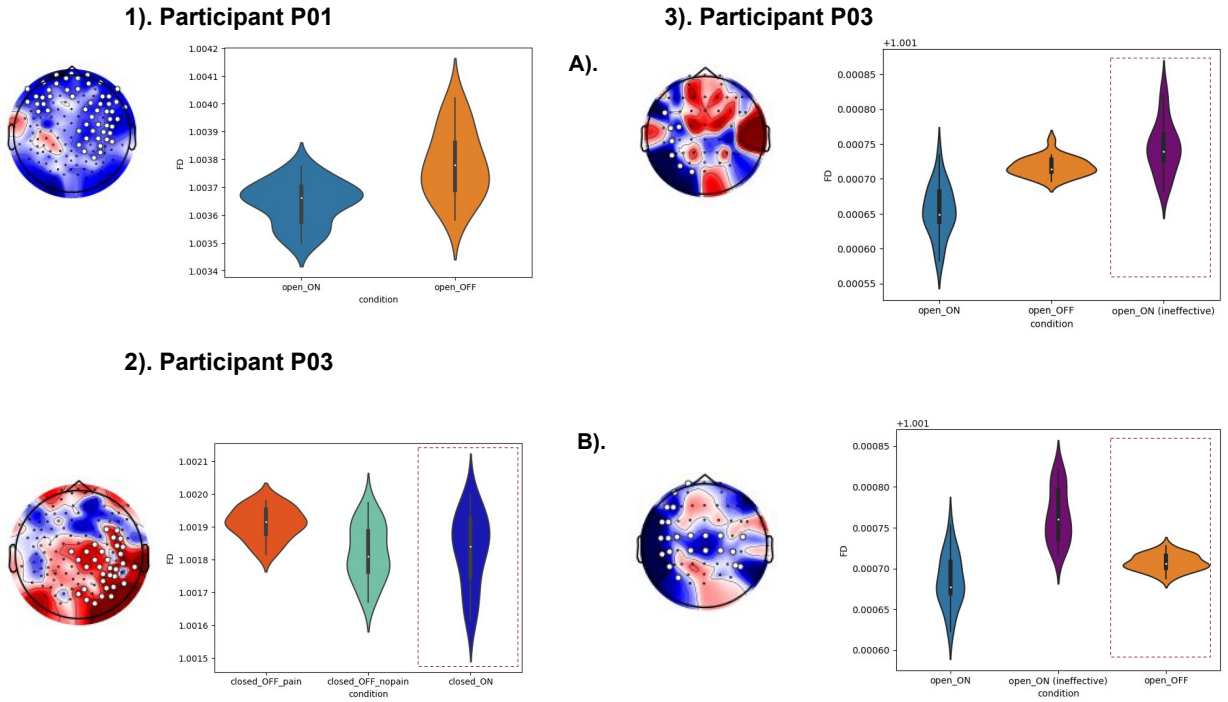

Figure 8: The analysis of fractal dimensions. Clusters with significant across-condition differences are shown. EEG channels, forming the clusters with significant differences, are marked with white dots. Scalp topographies depict t-values. The dashed rectangles represent the conditions which were not entered in the statistical analysis

.

reflecting idle state of sensory and motor systems, in pain conditions (Simis et al., 2022b; Teixeira et al., 2021). Additionally, neurofeedback aimed at increasing the low-beta oscillations is effective to treat chronic neuropathic pain (Hassan et al., 2015; Vučković et al., 2019). The mechanisms underlying the interrelation between beta rhythm and nociception could include GABAergic signaling (Barr et al., 2013). In this interpretation, pain is caused by an imbalance between excitation and inhibition with a bias towards excitation, resulting in a reduction of inhibitory input mediated by GABAergic neursons. Since the mechanisms of beta and gamma oscillations essentially depend on the inhibitory interneurons (Baumgarten et al., 2016), beta power could be considered as an indicator of GABAergic activity. Following this argumentation, the increase in beta power observed in our study could indicate facilitation of GABAergic activation by neurostimulation.

An alpha peak was absent in patient P02 spectra, so changes in alpha activity are unclear in this peculiar case. Patient P03 had a spectral peak at the alpha frequency. Although the effects of SCS in this patient were confounded with the effects of medication, changes in alpha power did occur after SCS was turned on. In the eyes-closed condition, this was an increase in alpha power accompanied by a decrease in theta power. This result is consistent with the previously assessed resting-state spectral characteristics during the application of SCS (Witjes et al., 2023), where several studies reported increase of alpha power. In addition to the possible effect of the medication, differences in the alpha-power patterns in patients P01 and P03, could have been related to stimulation type (PNS versus SCS) and the specifics of stimulation patterns. Burst-stimulation in patient P01 could have had an excitatory effect coupled to a decrease in alpha oscillations, while tonic stimulation in patient P03 could have inhibitory effect resulting in an increase in alpha power (Goudman et al., 2020).

Our interpretation that changes in EEG spatio-spectral characteristics reflected the level of PLP is supported by the observation of gradual changes in the EEG spectral characteristics after neurostimulation was turned off or on and PLP changed gradually. In patient P01, alpha power was increasing and low beta power was decreasing after PNS was turned off and PLP was intensifying. Conversely, after PNS was turned on, PLP was decreasing in patient P01 and alpha power was decreasing and beta power was increasing. Gradual changes in EEG patterns were observed in patient P02, as well. Theta power was increasing as PLP was intensifying after TENS was turned off, and theta power was decreasing after TENS was turned back on, which relieved PLP. This capacity of our approach to not only distinguish between the

presence and absence of pain based on EEG signals but also estimate the gradual changes in PLP is a valuable outcome for the development of prediction systems within the context of closed-loop neurostimulation systems.

The patient-specific variations in the EEG spectral characteristics highlight the need for a comprehensive understanding of each patient's spectral profile. They also present a challenge in obtaining universal markers of PLP and its suppression by neurostimulation. Yet, FD, the metric of signal complexity had similar trends for all patients. An increase in FD on the side contralateral to the amputation was associated with the presence of PLP, while a decrease in FD on the contralateral side was associated with PLP suppression by an effective neurostimulation. This suggests that FD could serve as a valuable and standardized metric for assessing pain and evaluating the impact of neurostimulation. There is no explicit indication of whether absolute increase or decrease in complexity measures corresponds to normalization of CNS activity. It was proposed that the deviation from an 'optimal variability' could become a criterion for the presence of a disorder (Lau et al., 2022), and the estimation of ranges of complexity measures of brain activity in healthy people and patients with neuropathic pain could form a distinct direction of research.

The main limitation of the study is that the number of participants and heterogeneity of their symptoms and response to the treatment does not allow for general conclusions. A larger sample of participants with more similar symptoms and therapeutic strategies would increase the reliability of the results. The other restrictions of the current design include possible overlap between EEG spectral signatures of conscious sensory experiences resulting from neurostimulation and PLP. This aspect should be controlled with sham stimulation at the same location but another parameters which do not induce pain relief. In our study we analyzed the paradigm with an ineffective stimulation, as it followed the therapeutic search for the effective treatment and did not include this scenario as a control condition for each of the patient.

The other methodological limitation is that the naturalistic experiments with neurostimulation and PLP suppression are associated with the recording of resting-state EEG data, which is not stable by its nature and is not as robust as evoked responses with well-known components calculated from the averaged trials. Indeed, it would be possible to evaluate context-dependent evoked responses to repetitive stimulation, but this paradigm creates the risks for sensory habituation and the observed changes of evoked responses may not reflect the changes in pain intensity (although it is possible to add sham stimulation as a control for this case, as well).

The other limitation is that stimulation-induced sensations could inadvertently compete with the intended pain suppression mechanisms. Addressing this limitation demands a comprehensive approach that considers not only pain reduction but also the broader neural consequences of neurostimulation.

The final limitation of the study is that multimodal nature of pain implies the involvement of multiple cortical regions, and the given the experimental design does not directly address or modulate the activity of the possible regions of interest (e. g. phantom limb representation in sensorimotor cortex, integrative nodes of nociception in insula, operculum, etc.). The use of high-density EEG partly solves this problem, as its high spatial resolution allows for implementing signal decomposition techniques and analyze data-driven regions of interest. Yet, additional preliminary mapping of the areas corresponding to phantom limb representation in the brain of given patient could be beneficial.

Despite the mentioned limitations, our results are generally in line with the previous studies, particularly regarding the consideration of the lower-frequency oscillations (theta and alpha) as markers of PLP and of the beta oscillations as a marker of pain-relieving neurostimulation. Taken together, these findings will likely contribute to the development of closed-loop systems for PLP suppression.

Acknowledgements

This work was supported by the Russian Science Foundation under grant № 21-75-30024.

Declarations of interest

AB, YM, and MS are employees of Motorica LLC, other authors declare that they have no known competing financial interests or personal relationships that could have appeared to influence the work reported in this paper. Motorica LLC is a private company, developing and producing functional prosthetics of upper limbs.

References

Alviar, M. J. M., Hale, T., and Lim-Dungca, M. (2016). Pharmacologic interventions for treating phantom limb pain. *Cochrane database of systematic reviews*, (10).

Barr, M. S., Farzan, F., Davis, K. D., Fitzgerald, P. B., and Daskalakis, Z. J. (2013). Measuring gabaergic inhibitory activity with tms-eeg and its potential clinical application for chronic pain. *Journal of Neuroimmune Pharmacology*, 8:535–546.

Baumgarten, T. J., Oeltzschner, G., Hoogenboom, N., Wittsack, H.-J., Schnitzler, A., and Lange, J. (2016). Beta peak frequencies at rest correlate with endogenous gaba+/cr concentrations in sensorimotor cortex areas. *PloS one*, 11(6):e0156829.

Bräscher, A.-K., Becker, S., Hoeppli, M.-E., and Schweinhardt, P. (2016). Different brain circuitries mediating controllable and uncontrollable pain. *Journal of Neuroscience*, 36(18):5013–5025.

Case, M., Shirinpour, S., Zhang, H., Datta, Y. H., Nelson, S. C., Sadak, K. T., Gupta, K., and He, B. (2017). Increased theta band eeg power in sickle cell disease patients. *Journal of pain research*, pages 67–76.

Dinh, S. T., Nickel, M. M., Tiemann, L., May, E. S., Heitmann, H., Hohn, V. D., Edenharter, G., Utpadel-Fischler, D., Tölle, T. R., Sauseng, P., et al. (2019). Brain dysfunction in chronic pain patients assessed by resting-state electroencephalography. *Pain*, 160(12):2751.

Fallon, N., Chiu, Y., Nurmikko, T., and Stancak, A. (2018). Altered theta oscillations in resting eeg of fibromyalgia syndrome patients. *European journal of pain*, 22(1):49–57.

Goudman, L., Linderoth, B., Nagels, G., Huysmans, E., and Moens, M. (2020). Cortical mapping in conventional and high dose spinal cord stimulation: an exploratory power spectrum and functional connectivity analysis with electroencephalography. *Neuromodulation: Technology at the Neural Interface*, 23(1):74–81.

Gramfort, A., Luessi, M., Larson, E., Engemann, D. A., Strohmeier, D., Brodbeck, C., Goj, R., Jas, M., Brooks, T., Parkkonen, L., et al. (2013). Meg and eeg data analysis with mne-python. *Frontiers in neuroscience*, page 267.

Hassan, M. A., Fraser, M., Conway, B. A., Allan, D. B., and Vuckovic, A. (2015). The mechanism of neurofeedback training for treatment of central neuropathic pain in paraplegia: a pilot study. *BMC neurology*, 15:1–13.

Jeanmonod, D., Magnin, M., Morel, A., Siegemund, M., Cancro, A., Lanz, M., Llinás, R., Ribary, U., Kronberg, E., Schulman, J., et al. (2001). Thalamocortical dysrhythmia ii. clinical and surgical aspects. *Thalamus & Related Systems*, 1(3):245–254.

Lau, Z. J., Pham, T., Chen, S. A., and Makowski, D. (2022). Brain entropy, fractal dimensions and predictability: A review of complexity measures for eeg in healthy and neuropsychiatric populations. *European Journal of Neuroscience*, 56(7):5047–5069.

Limakatso, K., Bedwell, G. J., Madden, V. J., and Parker, R. (2020). The prevalence and risk factors for phantom limb pain in people with amputations: a systematic review and meta-analysis. *PloS one*, 15(10):e0240431.

Llinás, R. R., Ribary, U., Jeanmonod, D., Kronberg, E., and Mitra, P. P. (1999). Thalamocortical dysrhythmia: a neurological and neuropsychiatric syndrome characterized by magnetoencephalography. *Proceedings of the National Academy of Sciences*, 96(26):15222–15227.

Lyu, Y., Guo, X., Wang, Z., and Tong, S. (2016). Resting-state eeg network change in alpha and beta bands after upper limb amputation. In *2016 38th Annual International Conference of the IEEE Engineering in Medicine and Biology Society (EMBC)*, pages 49–52. IEEE.

Maris, E. and Oostenveld, R. (2007). Nonparametric statistical testing of eeg-and meg-data. *Journal of neuroscience methods*, 164(1):177–190.

McCormick, Z., Chang-Chien, G., Marshall, B., Huang, M., and Harden, R. N. (2014). Phantom limb pain: a systematic neuroanatomical-based review of pharmacologic treatment. *Pain medicine*, 15(2):292–305.

Melzack, R. and Wall, P. D. (1965). Pain mechanisms: A new theory: A gate control system modulates sensory input from the skin before it evokes pain perception and response. *Science*, 150(3699):971–979.

Mussigmann, T., Bardel, B., and Lefaucheur, J.-P. (2022). Resting-state electroencephalography (eeg) biomarkers of chronic neuropathic pain. a systematic review. *NeuroImage*, page 119351.

Nikulin, V. V., Nolte, G., and Curio, G. (2011). A novel method for reliable and fast extraction of neuronal eeg/meg oscillations on the basis of spatio-spectral decomposition. *NeuroImage*, 55(4):1528–1535.

Olesen, S. S., Hansen, T. M., Graversen, C., Steimle, K., Wilder-Smith, O. H., and Drewes, A. M. (2011). Slowed eeg rhythmicity in patients with chronic pancreatitis: evidence of abnormal cerebral pain processing? *European journal of gastroenterology & hepatology*, 23(5):418–424.

Osumi, M., Sano, Y., Ichinose, A., Wake, N., Yozu, A., Kumagaya, S.-I., Kuniyoshi, Y., Morioka, S., and Sumitani, M. (2020). Direct evidence of eeg coherence in alleviating phantom limb pain by virtual referred sensation: Case report. *Neurocase*, 26(1):55–59.

Petersen, B. A., Nanivadekar, A. C., Chandrasekaran, S., and Fisher, L. E. (2019). Phantom limb pain: peripheral neuromodulatory and neuroprosthetic approaches to treatment. *Muscle & nerve*, 59(2):154–167.

Petrosian, A. (1995). Kolmogorov complexity of finite sequences and recognition of different preictal eeg patterns. In *Proceedings eighth IEEE symposium on computer-based medical systems*, pages 212–217. IEEE.

Sarnthein, J., Stern, J., Aufenberg, C., Rousson, V., and Jeanmonod, D. (2006). Increased eeg power and slowed dominant frequency in patients with neurogenic pain. *Brain*, 129(1):55–64.

Shirvalkar, P., Prosky, J., Chin, G., Ahmadipour, P., Sani, O. G., Desai, M., Schmitgen, A., Dawes, H., Shanechi, M. M., Starr, P. A., et al. (2023). First-in-human prediction of chronic pain state using intracranial neural biomarkers. *Nature neuroscience*, pages 1–10.

Simis, M., Imamura, M., Pacheco-Barrios, K., Marduy, A., de Melo, P. S., Mendes, A. J., Teixeira, P. E., Battistella, L., and Fregni, F. (2022a). Eeg theta and beta bands as brain oscillations for different knee osteoarthritis phenotypes according to disease severity. *Scientific reports*, 12(1):1480.

Simis, M., Pacheco-Barrios, K., Uygur-Kucukseymen, E., Castelo-Branco, L., Battistella, L. R., and Fregni, F. (2022b). Specific electroencephalographic signatures for pain and descending pain inhibitory system in spinal cord injury. *Pain Medicine*, 23(5):955–964.

Teixeira, M., Mancini, C., Wicht, C. A., Maestretti, G., Kuntzer, T., Cazzoli, D., Mouthon, M., Annoni, J.-M., and Chabwine, J. N. (2021). Beta electroencephalographic oscillation is a potential gabaergic biomarker of chronic peripheral neuropathic pain. *Frontiers in neuroscience*, 15:594536.

van den Broeke, E. N., Wilder-Smith, O. H., van Goor, H., Vissers, K. C., and van Rijn, C. M. (2013). Patients with persistent pain after breast cancer treatment show enhanced alpha activity in spontaneous eeg. *Pain medicine*, 14(12):1893–1899.

Vanneste, S., Ost, J., Van Havenbergh, T., and De Ridder, D. (2017). Resting state electrical brain activity and connectivity in fibromyalgia. *PloS one*, 12(6):e0178516.

Vase, L., Egsgaard, L. L., Nikolajsen, L., Svensson, P., Jensen, T. S., and Arendt-Nielsen, L. (2012). Pain catastrophizing and cortical responses in amputees with varying levels of phantom limb pain: a high-density eeg brain-mapping study. *Experimental brain research*, 218(3):407–417.

Vučković, A., Altaleb, M. K. H., Fraser, M., McGeady, C., and Purcell, M. (2019). Eeg correlates of self-managed neurofeedback treatment of central neuropathic pain in chronic spinal cord injury. *Frontiers in Neuroscience*, 13:762.

Walsh, E., Long, C., and Haggard, P. (2015). Voluntary control of a phantom limb. *Neuropsychologia*, 75:341–348.

Wang, W.-e., Roy, A., Misra, G., Ho, R. L., Ribeiro-Dasilva, M. C., Fillingim, R. B., and Coombes, S. A. (2019). Altered neural oscillations within and between sensorimotor cortex and parietal cortex in chronic jaw pain. *NeuroImage: Clinical*, 24:101964.

Witjes, B., Ottenheym, L. A., Huygen, F. J., and de Vos, C. C. (2023). A review of effects of spinal cord stimulation on spectral features in resting-state electroencephalography. *Neuromodulation: Technology at the Neural Interface*, 26(1):35–42.

Zebhauser, P. T., Hohn, V. D., and Ploner, M. (2023). Resting-state electroencephalography and magnetoencephalography as biomarkers of chronic pain: a systematic review. *Pain*, 164(6):1200.